arXiv:1509.09082v2 [physics.class-ph] 11 Oct 2016

Jean-Guy Caputo
*INSA de Rouen, France*

Denys Dutykh
*CNRS, Université Savoie Mont Blanc, France*

Bernard Gleyse
*INSA de Rouen, France*

# Coupling conditions for the nonlinear shallow water equations in forks

arXiv.org / HAL

Last modified: October 12, 2016

# Coupling conditions for the nonlinear shallow water equations in forks

Jean-Guy Caputo, Denys Dutykh*, and Bernard Gleyse

Abstract. We study numerically and analytically how nonlinear shallow water waves propagate in a fork. Using a homothetic reduction procedure, conservation laws and numerical analysis in a 2D domain, we obtain simple angle dependent coupling conditions for the water height and the velocity. These agree semi-quantitatively with the full numerical solutions for different geometries.

**Key words and phrases:** Networks; shallow water equations; nonlinear wave equations

**MSC:** [2010] 35Qxx (primary), 35R02 (secondary)
**PACS:** [2010] 47.35.Bb (primary), 47.15.gm (secondary)

*Key words and phrases.* Networks; shallow water equations; nonlinear wave equations.
* Corresponding author.

Contents

**1 Introduction . . . . . 5**

**2 The nonlinear shallow water equations . . . . . 6**

2.1 Conserved quantities . . . . . 7

**3 The different fork geometries . . . . . 8**

3.1 The elbow . . . . . 8

3.2 The branch . . . . . 8

**4 Reduction for a class of scalar nonlinear wave equations . . . . . 9**

**5 Reduction of the shallow water equations . . . . . 10**

5.1 Mass flux . . . . . 10

5.2 Energy flux . . . . . 11

5.3 Momentum flux for a general fork . . . . . 11

5.4 Momentum flux for the $T-$fork . . . . . 12

**6 Numerical method for solving the 2D shallow water equations . . . . . 13**

6.1 Wave incident into branch 1 . . . . . 15

6.2 Wave incident into branch 3 . . . . . 17

6.3 Wave incident into branch 1 for a $Y-$geometry . . . . . 21

**7 Conclusion . . . . . 22**

Acknowledgments . . . . . 23

**References . . . . . 23**

# 1. Introduction

To study the propagation of nonlinear waves in networks, a first step is to consider a simple fork as a model of elementary junctions. Another natural simplification is to reduce the problem from a 2D partial differential equation to a 1D effective partial differential equation with adequate coupling conditions at the interfaces. Recently we [2] introduced a homothetic reduction [2] where we average the operator over the fork region and consistently take the limit when the width tends to zero. For the sine–Gordon nonlinear wave equation, this gave the right interface conditions for the 1D model. The energy time plots for the 2D system and the 1D effective model agreed very well. The angle of the fork did not appear to play any significant role.

For classical hydrodynamics, the situation is not so simple. The angle in the fork sets the forces experienced by the pipes and controls the amount of mass going in each branch of the fork, see [11]. When considering networks of rivers, many authors, for example [17] and [10] assume continuity of the water height and continuity of the flux so that the angle of the fork does not come in. Recently, Herty & Seaïd [8] compared 2D solutions with solutions of a 1D effective model. They used damping in their equations and did not address the angle issue. While damping exists in real situations it breaks the symmetries of the equations. In the close context of gas dynamics, Holden & Risebro [9] studied a 1D system of conservation laws with a Dirac delta-function modeling an elbow in the pipe. For shocks they showed that the problem has a unique solution for given left and right densities and velocities for angles smaller than $\pi$. For the subsonic case, Colombo & Garavello [4] assuming conservation of the linear momentum showed the well-posedness of the Cauchy problem for a junction. These studies point out at the importance of the angle; the energy entering a branch can vary from 20% to 50% depending on the angle of the branch with the main branch. Another example is two dimensional traffic flow, see the review by Bellomo & Dogbé [1], there the angle of the intersections will also control the flow. It is then crucial to provide the 1D model with coupling conditions that reflect this dependence.

A few authors have addressed the problem. Schmidt [13] studied the 2D connection between 1D channels; there no assumption is made on the size of the connecting domain. The flow in the junction is assumed linear. The authors use a variational method: the solution is taken as a superposition of fields. The final result is a system of ordinary differential equations for the values at the ends of the branches coupled to the shallow water PDEs. Despite its formal beauty, it remains difficult to handle and does not give a simple picture. Another recent study by Nachbin & Simões [12] on the dispersive shallow water equations transforms the fork into a rectangle with a cut using a conformal map. The 2D PDE in this rectangle is then averaged transversally to obtain a 1D model whose solutions agree remarkably well with the ones of the original 2D model for small fork angles. The 1D model also gives interface conditions, based on the averaged Jacobian of the transformation; these generalize the ones of Stoker. These coupling conditions contain

the angle dependance implicitly through the JACOBIAN of the conformal map; they are difficult to generalize to an arbitrary angle.

In this article, using conservation laws, we obtain simple and explicit coupling conditions that depend on the angle. We can then use these to connect one dimensional models for the branches. To derive the coupling conditions, we revisit the general problem using our homothetic reduction procedure. We consider a general class of scalar nonlinear wave equations, for example the 2D sine–GORDON equation or the 2D reaction-diffusion equation with homogeneous Neumann boundary conditions and the shallow water equations. For the first model, the reduction is natural and yields simple jump conditions: continuity of the field and continuity of the gradient (KIRCHOFF's law). The angle of the channels does not play any role in the reduction and we obtain the same 1D effective model for any $n$ channel configuration, confirming the results of [2]. For the shallow water equations, the reduction gives mass and energy couplings; the former is the flux conservation used by STOKER. The reduction of the momenta shows additional terms appearing; these contain the effect of the boundary and therefore the angular dependance. We illustrate this on a simple $T-$fork geometry and input the wave on two different branches to analyze the angular dependence of the solution. Using the 2D numerical solution together with the results of the reduction, we obtain new explicit coupling conditions at the interface that depend on the angle configuration. These give a consistent 1D effective model. The procedure is also applied to a $Y-$fork and again we obtain explicit coupling conditions.

The article is organized as follows. After recalling the shallow water equations and their conserved quantities in Section 2, we present the geometries in Section 3. Section 4 shows the straightforward reduction of a general class of nonlinear wave equations. Section 5 presents the reduction for the shallow water equations; while the results are simple for the mass and the energy, they are complex for the momenta. A detailed analysis of the two main branch dynamical problems is presented in Section 6 together with the results for the $Y-$branch; for these geometries we give the coupling conditions and compare them to the full numerical solutions. Conclusions are given in Section 7.

## 2. The nonlinear shallow water equations

The shallow water equations in a 2D domain can be written in terms of the fluid velocity $\mathbf{u}(x,t)$

$$\mathbf{u} \;=\; (u,\, v)^{\top}\,.$$

and the water height $h(x,t)$ [17]. They read

$$h_t \;+\; \nabla\cdot(h\mathbf{u}) \;=\; 0\,, \tag{2.1}$$

$$(hu)_t \;+\; \nabla\cdot\begin{pmatrix} hu^2 \;+\; \frac{gh^2}{2} \\ huv \end{pmatrix} \;=\; 0\,, \tag{2.2}$$

$$(hv)_t \;+\; \nabla\cdot\begin{pmatrix} huv \\ hv^2 \;+\; \frac{gh^2}{2} \end{pmatrix} \;=\; 0\,, \tag{2.3}$$

where $g$ is the gravity acceleration. The wall boundary condition is

$$\mathbf{u} \cdot \mathbf{n} \;=\; 0\,. \tag{2.4}$$

We assume an even bottom of the channels.

## 2.1. Conserved quantities

We first recall the conserved quantities. Integrating equations (2.1) – (2.3) over a 2D closed domain $\Omega$ and using the boundary condition (2.4) we get

$$\partial_t \int_\Omega h \;\mathrm{d}x\,\mathrm{d}y \;=\; 0\,, \tag{2.5}$$

$$\partial_t \int_\Omega hu \;\mathrm{d}x\,\mathrm{d}y \;+\; \int_{\partial\Omega} \frac{gh^2}{2}\, n_x \;\mathrm{d}s \;=\; 0\,, \tag{2.6}$$

$$\partial_t \int_\Omega hv \;\mathrm{d}x\,\mathrm{d}y \;+\; \int_{\partial\Omega} \frac{gh^2}{2}\, n_y \;\mathrm{d}s \;=\; 0\,. \tag{2.7}$$

The first conserved quantity is the integral of the water elevation

$$M \;=\; \int_\Omega h \;\mathrm{d}x\mathrm{d}y\,.$$

The total $x$ and $y$ momenta

$$P_x \;=\; \int_\Omega hu \;\mathrm{d}x\,\mathrm{d}y\,, \qquad P_y \;=\; \int_\Omega hv \;\mathrm{d}x\,\mathrm{d}y$$

are not conserved in the geometries that we will consider. However the flux relations (2.6), (2.6) associated with the momenta always hold.

A flux relation that can be deduced from the conservation laws is the total energy flux where the total energy density is

$$e \;=\; \frac{1}{2}\left[\, gh^2 \;+\; (u^2 \;+\; v^2)\, h \,\right]\,. \tag{2.8}$$

From (2.1) – (2.3) it can be seen that

$$e_t \;+\; \nabla \cdot \left[ (e \;+\; \frac{gh^2}{2})\, \mathbf{u} \right] \;=\; 0\,. \tag{2.9}$$

Integrating this relation over a volume $\Omega$ and assuming a localized wave such that $\mathbf{u}\cdot\mathbf{n} \;=\; 0$ on $\partial\Omega$, one obtains

$$0 \;=\; \frac{\mathrm{d}E}{\mathrm{d}t} \;=\; \frac{\mathrm{d}}{\mathrm{d}t} \int_\Omega e \;\mathrm{d}x\,\mathrm{d}y\,,$$

*i.e.* the conservation of the energy of the wave in a region bounded by impenetrable walls.

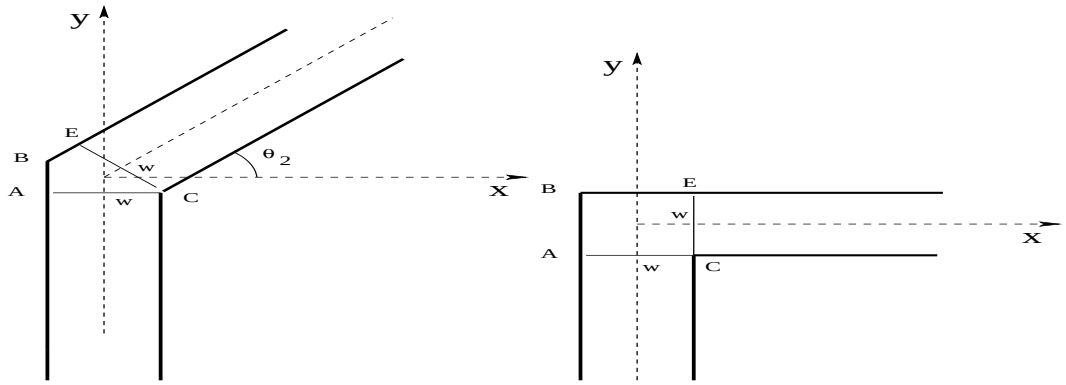


**Figure 1.** *A simple elbow geometry with an arbitrary angle (left) and a right angle (right).*

## 3. The different fork geometries

To reduce the 2D problem to a 1D effective problem, we proceed as in [2] and integrate the operators on the different subdomains corresponding to the defect. Then we examine the behavior of the different terms as $w$, the width of the branches, goes to zero. It is important that the domains that we consider behave in a regular way as we shrink $w$ homothetically to zero, [7]. We will have a consistent one-dimensional model if the limit is well defined.

### 3.1. The elbow

A first simple domain is the elbow shown in Fig. 1. The two branches have a width $w$. The defect region has two inside components $CA$ and $BC$ of length $w$. The other components AB and BE scale like $w$ as can be seen from the coordinates of $A$, $C$ and $B$. Then when $w \to 0$, the domain reduces to two lines. In Fig. 1 the left panel is a configuration with an arbitrary angle and the right panel shows the right angle configuration for which the calculations are easier due to our choice of the CARTESIAN coordinates.

### 3.2. The branch

The elbow is a simple configuration which shows how the angle influences the coupling conditions. Here we are mostly interested in branches or forks as in Fig. 2. As for the elbow, these domains reduce to lines when $w \to 0$. The results obtained for the fork can be directly applied to the elbow by taking out the contribution from the 3rd branch.

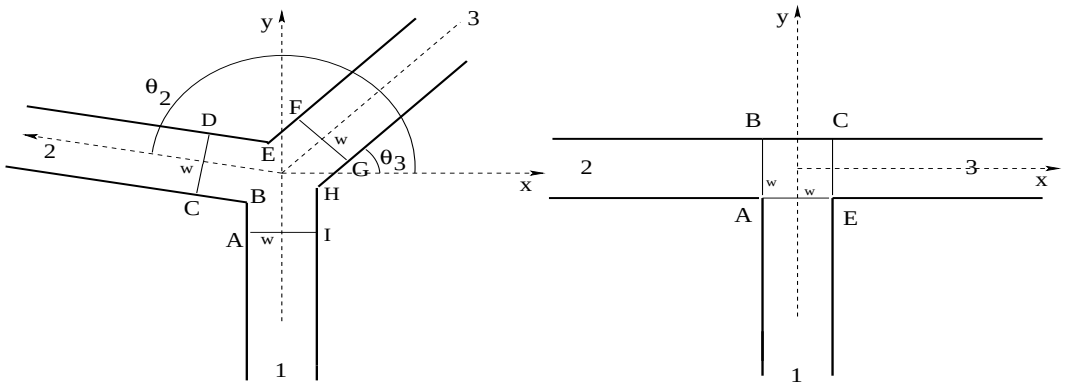


**Figure 2.** *A fork geometry with arbitrary angles (left) and with right angles (right).*

## 4. Reduction for a class of scalar nonlinear wave equations

Before giving the results for the shallow water equations, we analyze the simpler case of a class of scalar nonlinear wave equations. The 2D nonlinear wave equation we consider is a large class that includes hyperbolic wave equations like the sine–GORDON equation as well as reaction diffusion equations like the FISHER equation. It can be written

$$\alpha\, u_{tt} \;+\; \beta\, u_t \;-\; \Delta u \;=\; N(u)\,, \tag{4.1}$$

where $u(x, y, t)$ is a scalar, $\Delta$ is the usual 2D LAPLACIAN and where $N(u)$ is a nonlinearity not containing derivatives. The boundary condition on the lateral domain is of NEUMANN type

$$\partial_n u \;=\; \boldsymbol{\nabla} u \cdot \mathbf{n} \;=\; 0\,. \tag{4.2}$$

The reduction of this class of scalar nonlinear wave equations is much simpler than the one of the shallow water equations. In all cases we get an effective 1D model. To illustrate this consider the asymmetric $Y-$branch shown in the left panel of Fig. 2. A first assumption is the continuity of $u$ which is obvious for the 2D operator. The other condition comes from the integration of the operator (4.1) on the fork domain. We get

$$\int [\alpha u_{tt} \;+\; \beta u_t \;-\; N(u)]\, \mathrm{d}x\, \mathrm{d}y \;-\; \int_{ABCDEFGHIA} (\nabla u) \cdot \mathbf{n}\, \mathrm{d}s \;=\; 0\,.$$

The first integral is of order $\mathcal{O}(w^2)$. On the exterior boundaries, $(\nabla u) \cdot \mathbf{n} \;=\; 0$ so the line integral reduces to

$$\int_{BC} \ldots \;+\; \int_{EF} \ldots \;+\; \int_{AG} \ldots$$

which are $\mathcal{O}(w)$. We then obtain for $w \;\to\; 0$

$$-\,\partial_s u_1 \;+\; \partial_s u_2 \;+\; \partial_s u_3 \;=\; 0\,, \tag{4.3}$$

where $u_i$, $i \;=\; 1 \ldots 3$ are respectively the values of the field at the end of branch 1 $(AG)$ and at the beginning of branches 2 $(EF)$ and 3 $(BC)$. Relation (4.3) is KIRCHHOFF's law

[2]. In this case the angle does not play a rôle. When the widths of the branches are not equal, the KIRCHOFF relation becomes

$$-\,w_1\,\partial_s u_1 \;+\; w_2\,\partial_s u_2 \;+\; w_3\,\partial_s u_3 \;=\; 0\,. \tag{4.4}$$

The validity of the reduction was confirmed numerically in [2] where we compared the solutions of the 1D model with the ones of the 2D original model. We refer the reader to [2] for more details.

# 5. Reduction of the shallow water equations

The shallow water equations cannot be reduced so simply as the nonlinear scalar wave equation. In fact, it is not clear what are the right interface conditions that should be implemented for a 1D effective model. To understand the problem, we proceed as in [2], integrate the operator on the bifurcation region and consider the limit of small transverse width $w$.

## 5.1. Mass flux

Integrating the equation (2.1) over the region $ABCDEFGHIA$ yields

$$\int_{ABCDEFGHIA} h_t \,\mathrm{d}x\mathrm{d}y \;+\; \int_{ABCDEFGHIA} h\;\mathbf{u}\cdot\mathbf{n}\,\mathrm{d}s \;=\; 0\,.$$

Because of the boundary condition $\mathbf{u}\cdot\mathbf{n} \;=\; 0$ on $ABC$, $DEF$ and $GHI$ the expression above reduces to

$$\int_{ABCDEFGHIA} h_t \,\mathrm{d}x\,\mathrm{d}y + \int_{AI} h\;\mathbf{u}\cdot\mathbf{n}\,\mathrm{d}s \;+\; \int_{CD} h\;\mathbf{u}\cdot\mathbf{n}\,\mathrm{d}s \;+\; \int_{FG} h\;\mathbf{u}\cdot\mathbf{n}\,\mathrm{d}s \;=\; 0\,.$$

The first integral is $\mathcal{O}(w^2)$ while the two other integrals are $\mathcal{O}(w)$. Dividing the equation by $w$ and taking the limit $w \;\to\; 0$ we get from these three terms

$$-\,h_1\,u_1^{\parallel} \;+\; h_2\,u_2^{\parallel} \;+\; h_3 u_3^{\parallel} \;=\; 0\,, \tag{5.1}$$

where we have introduced the local branch-oriented velocities $u^{\parallel}$, $u^{\perp}$ and the indices 1, 2 and 3 refer to the branches. Of course, when the transverse widths $w_1$, $w_2$, $w_3$ are different, with the condition that the ratios $w_2/w_1$, $w_3/w_1$ remain finite, the relation (5.1) becomes

$$-w_1\,h_1\,u_1^{\parallel} \;+\; w_2\,h_2\,u_2^{\parallel} \;+\; w_3\,h_3\,u_3^{\parallel} \;=\; 0\,.$$

## 5.2. Energy flux

The energy flux (2.9) can be consistently reduced to a 1D relation. As for the mass relation, we integrate equation (2.8) over the region $ABCDEFGHIA$ to obtain

$$\int_{ABCDEFGHIA} e_t \,\mathrm{d}x\,\mathrm{d}y \;+\; \int_{ABCDEFGHIA} \Big(e \;+\; \frac{gh^2}{2}\Big)\,\mathbf{u}\cdot\mathbf{n}\,\mathrm{d}s \;=\; 0\,.$$

Because of the boundary condition $\mathbf{u}\cdot\mathbf{n} \;=\; 0$ on $ABE$, the expression above reduces to

$$\begin{aligned}\int_{ABCDEFGHIA} e_t \,\mathrm{d}x\,\mathrm{d}y \;+\; \int_{AI} \Big(e \;+\; \frac{gh^2}{2}\Big)\,\mathbf{u}\cdot\mathbf{n}\,\mathrm{d}s \\ +\; \int_{CD} \mathrm{d}s\,\Big(e \;+\; \frac{gh^2}{2}\Big)\,\mathbf{u}\cdot\mathbf{n}\,\mathrm{d}s \;+\; \int_{FG} \mathrm{d}s\,\Big(e \;+\; \frac{gh^2}{2}\Big)\,\mathbf{u}\cdot\mathbf{n}\,\mathrm{d}s \;=\; 0\,.\end{aligned}$$

The first integral is $\mathcal{O}(w^2)$ while the three other integrals are $\mathcal{O}(w)$. Dividing the equation by $w$ and taking the limit $w \;\to\; 0$ we get from these three terms

$$-\Big(e_1 \;+\; \frac{gh_1^2}{2}\Big)\,u_1^{\parallel} \;+\; \Big(e_2 \;+\; \frac{gh_2^2}{2}\Big)u_2^{\parallel} \;+\; \Big(e_3 \;+\; \frac{gh_3^2}{2}\Big)u_3^{\parallel} \;=\; 0\,. \tag{5.2}$$

To conclude, equation (2.1) gives in the 1D limit, the conservation of mass (5.1). The same happens for the energy flux (2.9) which yields (5.2). The natural matching conditions for 1D shallow water equations on a network are then

$$-\,h_1\,u_1^{\parallel} \;+\; h_2 u_2^{\parallel} \;+\; h_3 u_3^{\parallel} \;=\; 0\,, \tag{5.3}$$

$$-u_1^{\parallel}\Big(gh_1^2 \;+\; h_1\frac{{u_1^{\parallel}}^2}{2}\Big) \;+\; u_2^{\parallel}\Big(gh_2^2 \;+\; h_2\frac{{u_2^{\parallel}}^2}{2}\Big) \;+\; u_3^{\parallel}\Big(gh_3^2 \;+\; h_3\frac{{u_3^{\parallel}}^2}{2}\Big) \;=\; 0\,. \tag{5.4}$$

For the mass and the energy conservation laws, we have a similar situation to the one of the nonlinear scalar wave equation, the angles of the fork do not play any role. Finally note that the Stoker interface conditions

$$h_1 \;=\; h_2 \;=\; h_3\,, \tag{5.5}$$

$$-h_1\,u_1^{\parallel} \;+\; h_2\,u_2^{\parallel} \;+\; h_3\,u_3^{\parallel} \;=\; 0\,, \tag{5.6}$$

are not consistent with the energy flux relation (5.4).

## 5.3. Momentum flux for a general fork

Contrary to the mass and the energy, the momentum equations (2.2) – (2.3) cannot be consistently reduced to a 1D condition. At a first observation it appears that the two components of the momentum are generally not conserved in a bifurcation or a fork. This is true if the problem is one dimensional. In reality, there are recirculations of the fluid and these transform the momentum from one direction to another. The conservation laws (2.2) – (2.3) hold nevertheless. We will first treat the general fork shown in the left panel of Fig. 2.

Integrating $u$ momentum equation (2.2) over the domain $ABCDEFGHIA$ yields

$$\int_{ABCDEFGHIA} (hu)_t \, \mathrm{d}x \, \mathrm{d}y + \int_{ABCDEFGHIA} \begin{pmatrix} hu^2 + \frac{gh^2}{2} \\ huv \end{pmatrix} \cdot \mathbf{n} \, \mathrm{d}s = 0 \,,$$

where the first integral is a surface integral and the second one a line integral. The $\mathcal{O}(w)$ terms (line integrals) reduce to

$$\begin{aligned} &\left(-|AB| g \frac{h_{AB}^2}{2} + |HI| g \frac{h_{HI}^2}{2}\right) + \sin\theta_3 \left(|DE| g \frac{h_{DE}^2}{2} - |BC| g \frac{h_{BC}^2}{2}\right) \\ &+ \sin\theta_2 \left(|EF| g \frac{h_{EF}^2}{2} - |HG| g \frac{h_{HG}^2}{2}\right) + |CD| \left[(hu^2 + g\frac{h^2}{2}) \cos\theta_3 + huv \sin\theta_3\right] \\ &+ |FG| \left[(hu^2 + g\frac{h^2}{2}) \cos\theta_2 + huv \sin\theta_2\right] = 0 \,. \end{aligned}$$

Noting that $u_2^{\parallel} = u\cos\theta_2 + v\sin\theta_2$ and similarly for $u_3^{\parallel}$ we get the final result

$$\begin{aligned} &\frac{g}{2}\left(-|AB| h_{AB}^2 + |HI| h_{HI}^2\right) + \frac{g}{2}\sin\theta_3 \left(|DE| h_{DE}^2 - |BC| h_{BC}^2\right) \\ &+ \frac{g}{2}\sin\theta_2 \left(|EF| h_{EF}^2 - |HG| h_{HG}^2\right) + |CD| \left[h_3 {u_3^{\parallel}}^2 + g\frac{{h_3}^2}{2}\right] \cos\theta_3 \\ &+ |FG| \left[h_2 {u_2^{\parallel}}^2 + g\frac{{h_2}^2}{2}\right] \cos\theta_2 = 0 \,, \end{aligned} \tag{5.7}$$

where we neglected the velocity components in the transverse directions, since they vanish in the limit $w \to 0$. Similarly for the $v$ momentum equation we obtain

$$\begin{aligned} &-\frac{g}{2}\cos\theta_3 \left(|DE| h_{DE}^2 - |BC| h_{BC}^2\right) - \frac{g}{2}\cos\theta_2 \left(|EF| h_{EF}^2 - |HG| h_{HG}^2\right) \\ &- |AI| \left[h_1 {u_1^{\parallel}}^2 + g\frac{{h_1}^2}{2}\right] + |CD| \left[h_3 {u_3^{\parallel}}^2 + g\frac{{h_3}^2}{2}\right] \sin\theta_3 \\ &+ |FG| \left[h_2 {u_2^{\parallel}}^2 + g\frac{{h_2}^2}{2}\right] \sin\theta_2 = 0 \,. \end{aligned} \tag{5.8}$$

## 5.4. Momentum flux for the $T-$fork

We illustrate this for the $T-$geometry (right panel of Fig. 2) because the calculations are simpler. Also, we will use this geometry to validate the approach numerically.

As above, we integrate equation (2.2) over the fork domain $ABCEA$

$$\int (hu)_t \, \mathrm{d}x \, \mathrm{d}y + \int_{ABCEA} \begin{pmatrix} hu^2 + \frac{h^2}{2} \\ huv \end{pmatrix} \cdot \mathbf{n} \, \mathrm{d}s = 0 \,.$$

The first term is $\mathcal{O}(w^2)$. The $\mathcal{O}(w)$ terms (line integrals) reduce to

$$-h_1\,u_1\,v_1 \;-\; (h_2\,u_2^2 \;+\; g\,\frac{h_2^2}{2}) \;+\; h_3\,u_3^2 \;+\; g\,\frac{h_3^2}{2} \;=\; 0\,. \tag{5.9}$$

Similarly for the $v$ momentum, we get

$$-h_1\,v_1^2 \;+\; g\,\frac{h_1^2}{2} \;-\; h_2\,u_2\,v_2 \;+\; g\,\frac{h_{23}^2}{2} \;+\; h_3\,u_3\,v_3 \;=\; 0\,, \tag{5.10}$$

where the term $h_{23}$ is an unknown value, which can be obtained by interpolation of $h_2$ and $h_3$; it represents the field $h$ on the side $BC$. The terms $u_1$, $v_2$, $v_3$ disappear in the limit $w \;\to\; 0$ so the final results are

$$h_2\,u_2^2 \;+\; g\,\frac{h_2^2}{2} \;+\; h_3\,u_3^2 \;+\; g\,\frac{h_3^2}{2} \;=\; 0\,. \tag{5.11}$$

$$-h_1\,v_1^2 \;+\; g\,\frac{h_1^2}{2} \;+\; g\,\frac{h_{23}^2}{2} \;=\; 0\,. \tag{5.12}$$

Contrary to the mass and energy which give clear jump conditions in the 1D limit (5.3), the relations for the momentum involve extra terms which need to be approximated. To understand how to proceed, we have solved numerically the 2D shallow water equations.

## 6. Numerical method for solving the 2D shallow water equations

For simplicity we concentrate on the $T-$geometry. To solve the equations (2.1) – (2.3), we choose as space unit the depth $d$. The time unit is $\sqrt{\frac{d}{g}}$. The variables and fields are rescaled as

$$x' \;=\; \frac{x}{d}\,,\quad t' \;=\; t\,\sqrt{\frac{g}{d}}\,,\quad h' \;=\; \frac{x}{d}\,,\quad u' \;=\; \frac{u}{\sqrt{gd}}\,. \tag{6.1}$$

This amounts to taking $d \;=\; 1\,,\, g \;=\; 1$ in (2.1) – (2.3).

We solve the nonlinear shallow water equations using a first order finite volume scheme on an unstructured triangular mesh produced with the `Gmsh` meshing software. This scheme is explained in detail in [6]. The typical size of the triangles is 0.02. For the time integration we use a variable order Adams–Bashforth–Moulton multistep solver (implemented in `Matlab` under `ode113` subroutine [16]). The relative and absolute tolerances were set to $10^{-5}$.

The initial condition is taken as a traveling solitary wave of velocity $c$. This is an exact solution for the mass conservation law. We use a solitary wave inspired by the [14, 15] theory. See [5] for the modern variational derivation.

$$h\,(x,\,y,\,t \;=\; 0) \;=\; d \;+\; a\,\mathrm{sech}^2\Big(\frac{1}{2}\,k\,(y \;-\; y_0)\Big) \;\equiv\; d \;+\; \eta\,(x,\,y,\,0)\,, \tag{6.2}$$

$$v\,(x,\,y,\,t \;=\; 0) \;=\; c\,\frac{\eta\,(x,\,y,\,0)}{d \;+\; \eta\,(x,\,y,\,0)}\,, \tag{6.3}$$

| *Type* | *known* | *unknown* |
|---|---|---|
| wave in branch 1 | $h_1$, $v_1$ | $h_2$, $u_2$, $h_3$, $u_3$ |
| wave in branch 3 | $h_3$, $u_3$ | $h_1$, $v_1$, $h_2$, $u_2$ |

**Table 1.** *The two different dynamic problems for the $T-$branch.*

where the speed is

$$c \;=\; \sqrt{g(d \;+\; a)}\,.$$

The other parameters are

$$g \;=\; 1\,, \quad k \;=\; 1\,, \quad d \;=\; 1\,, \quad a \;=\; 1.0\,, \quad x_0 \;=\; y_0 \;=\; 2.5\,.$$

The wave is chosen so that its extension $\frac{2}{k} \;=\; 2$ is much larger than the width $w$. The calculations were done for three different values of the width $w$, $w \;=\; 0.5\,, 0.25$ and $0.125$. The results are similar for these three values so that we will only present the results for $w \;=\; 0.125$.

The four equations obtained from integrating the operators for the mass, momentum and energy on the fork domain $ABCEA$ reduce to

$$\delta m \;\equiv\; -h_1\,v_1 \;-\; h_2\,u_2 \;+\; h_3\,u_3 \;=\; 0\,, \tag{6.4}$$

$$\delta p_x \;\equiv\; -\left(h_2\,u_2^2 \;+\; g\,\frac{h_2^2}{2}\right) \;+\; h_3\,u_3^2 \;+\; g\,\frac{h_3^2}{2} \;=\; 0\,, \tag{6.5}$$

$$\delta p_y \;\equiv\; -\left(h_1\,v_1^2 \;+\; g\,\frac{h_1^2}{2}\right) \;+\; g\,\frac{h_{23}^2}{2} \;=\; 0\,, \tag{6.6}$$

$$\delta e \;\equiv\; -v_1\left(gh_1^2 \;+\; h_1\frac{v_1^2}{2}\right) \;-\; u_2\left(gh_2^2 \;+\; h_2\,\frac{u_2^2}{2}\right) \;+\; u_3\left(gh_3^2 \;+\; h_3\frac{u_3^2}{2}\right) \;=\; 0\,, \tag{6.7}$$

where we introduced the residuals $\delta m\,,\ \delta p_x\,,\ \delta p_y$ and $\delta e\,$.

Two problems will be considered, whether we send the wave into branch 1 or branch 3. In these two problems, the number of unknowns is the same; see Table 1.

The wave mass and wave energy in each branch have been calculated. They are defined as

$$M_w \;=\; \int_\Omega (h \;-\; d)\;\mathrm{d}x\,\mathrm{d}y$$

$$E_w \;=\; \int_\Omega \frac{1}{2}\left[g(h \;-\; d)^2 \;+\; (u^2 \;+\; v^2)\,h\right]\;\mathrm{d}x\,\mathrm{d}y\,.$$

Energy will propagate very differently in problems 1 and 2. In the next sections we examine in detail the two types of problems and use the conservation laws to establish jump conditions for the 1D effective model.

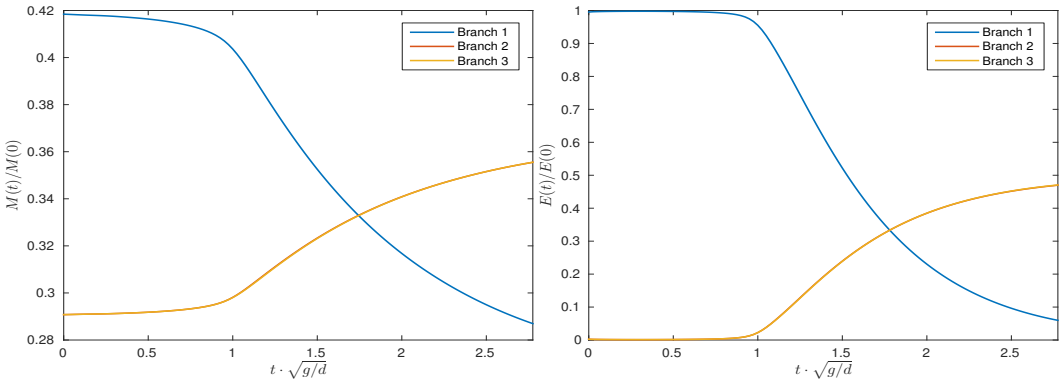


**Figure 3.** *Time evolution of the wave mass $M_w$ (left) and the wave energy $E_w$ (right) for a wave incident in branch* 1 .

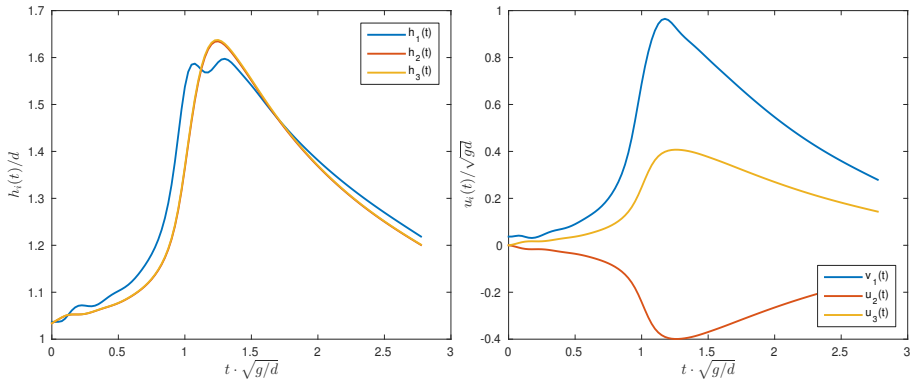


**Figure 4.** *Time evolution of the wave heights $h_1$, $h_2$, $h_3$ (left) and the wave speeds $v_1$, $u_2$, $u_3$ for a wave incident in branch* 1 .

## 6.1. Wave incident into branch 1

In this case, the wave in branch 1 will split up evenly between branches 2 and 3 which will receive 50% of the energy as shown on the right panel of Fig. 3. The wave mass goes from 0.42 in branch 1 to 0.35 in branches 2 and 3 ; the total mass is conserved so we have

$$0.42 \;-\; 0.28 \;=\; 0.14 \;=\; 2 \times (0.35 \;-\; 0.28)\,.$$

There is very little reflection for the wave amplitude we have considered, $a \;=\; 1$ . For larger amplitudes, we enter the shock regime and observe a significant reflection.

To verify the approximation given by the relations (6.4) – (6.7), we first computed the time evolution of the quantities $h_1$, $h_2$, $h_3$, $v_1$, $u_2$, $u_3$ from the 2D direct numerical simulations. We used a scattered linear interpolation to estimate the physical variables along the four different segments of the fork region from the unstructured triangular mesh data. The results are presented in Fig. 4.

| *time* | $\delta m/M$ | $\delta e/E$ |
|---|---|---|
| 0.75 | -0.03 | -0.03 |
| 1 | -0.226 | -0.37 |
| 1.25 | -0.096 | -0.23 |
| 1.5 | -0.04 | -0.13 |
| 1.8 | -0.02 | -0.07 |
| 2.5 | -0.004 | -0.015 |

**Table 2.** *The mass and energy residuals $\delta m$, $\delta e$ in the equations (6.4) – (6.7) for different times.*

As a first step towards model reduction, we validate our integral conservation laws using the 2D solution. In Table 2 we report the values of the left hand sides in the equations (6.4) – (6.7) for the mass and the energy. These have been normalized by the initial mass and initial energy which are respectively

$$M \;=\; 1.77\,, \qquad E \;=\; 2.37\,.$$

These results show that our approximation is valid most of the time except for the transient regime when the wave hits the wall. At that instant, the motion is significantly two dimensional so that an averaging procedure fails to capture the dynamics.

If we neglect the time instants when the 1D approximation breaks down, we can obtain interface conditions from (6.4) – (6.7). For that, we assume symmetry

$$h_2 \;=\; h_3\,, \qquad u_2 \;=\; -u_3\,.$$

We then get the two equations

$$2\,h_2\,u_2 \;=\; -h_1\,v_1\,, \tag{6.8}$$

$$2\,u_2\left(g h_2^2 \;+\; \frac{u_2^2}{2}\,h_2\right) \;=\; -v_1\left(g h_1^2 \;+\; \frac{v_1^2}{2}\,h_1\right). \tag{6.9}$$

The system reduces to the third degree equation

$$u_2{}^3 \;-\; (2\,g\,h_1 \;+\; v_1^2)\,u_2 \;-\; g\,h_1\,v_1 \;=\; 0\,, \tag{6.10}$$

whose solution in the limit $|u_2| \;\leqslant\; 1$ is

$$u_2 \;=\; -\,\frac{g\,h_1\,v_1}{2\,g\,h_1 \;+\; v_1^2}\,, \qquad h_2 \;=\; h_1 \;+\; \frac{v_1^2}{2g}\,. \tag{6.11}$$

An interesting observation is that among the three solutions of (6.10), we choose the one such that $u_2 \;\to\; 0$ and $h_2 \;\to\; 1$ when the wave has crossed the junction, *i.e.* when $v_1 \;\to\; 0$ and $h_1 \;\to\; 1$. For small $v_1$ we obtain $u_2 \;=\; -v_1/2$, which is the Stoker solution or steady state solution.

We can now proceed to check the estimates (6.11). For that we use the values $h_1$, $v_1$, $h_2$, $u_2$ from the simulations and compute the values from (6.11). Fig. 5 shows this comparison

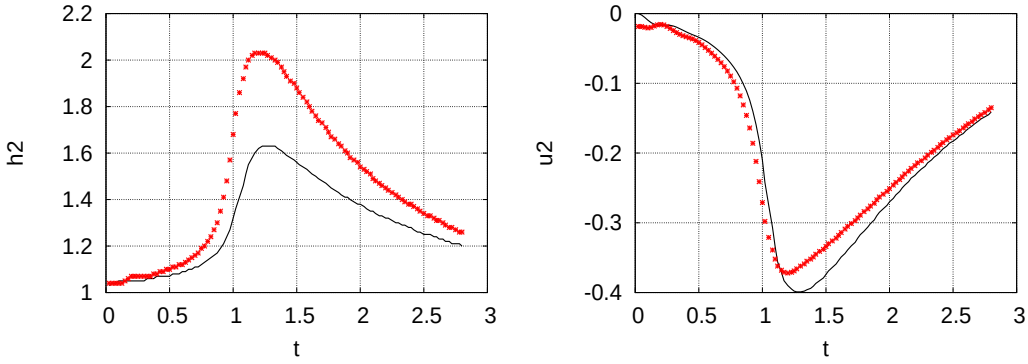


**Figure 5.** *Time evolution of the wave height $h_2$ (left) and the wave speed $u_2$ (right) for a wave incident in branch 1. The values from the 2D simulation are drawn in continuous line (black online) while the estimates (6.11) are in dashed line (red online).*

for $h_2$ (left panel) and $u_2$ (right panel) for different times. The "*exact*" values from the simulation are drawn in continuous line (black online) and the estimates (6.11) are in dashed line (red online). Clearly $h_2$ is overestimated, while $u_2$ agrees fairly well.

## 6.2. Wave incident into branch 3

For this configuration, about 70% of the wave energy will continue in branch 2, 20% will enter branch 1 and 10% will remain in branch 1, as shown in the right panel of Fig. 6. These ratios vary with the wave amplitude. For larger amplitudes, almost 100% passes into branch 2 . This confirms that that there is a strong angular dependence of the energy flow through the fork. The left panel shows the wave mass, 0.38 for branch 2, 0.34 for branch 1 . Again the mass is conserved because

$$0.42 \;-\; 0.28 \;=\; 0.14 \;=\; (0.38 \;-\; 0.28) \;-\; (0.34 \;-\; 0.28)\,.$$

When the wave is coming from branch 3 , an obvious solution is

$$v_1 \;=\; 0\,, \quad u_2 \;=\; u_3\,, \quad h_2 \;=\; h_3\,, \quad h_1 \;=\; h_2\,. \tag{6.12}$$

This is simplistic, in reality $v_1 \;\neq\; 0$ but remains small. As for problem 1, to understand this, we compute the time evolution of the quantities $h_1$, $h_2$, $h_3$, $v_1$, $u_2$, $u_3$ from the 2D direct numerical simulations. Here about 20% of the energy is transferred to branch 1. The results are presented in Fig. 7.

The quantity

$$h_{23}^2 \;\equiv\; \frac{1}{w} \int_{BC} h^2 \,\mathrm{d}s\,, \tag{6.13}$$

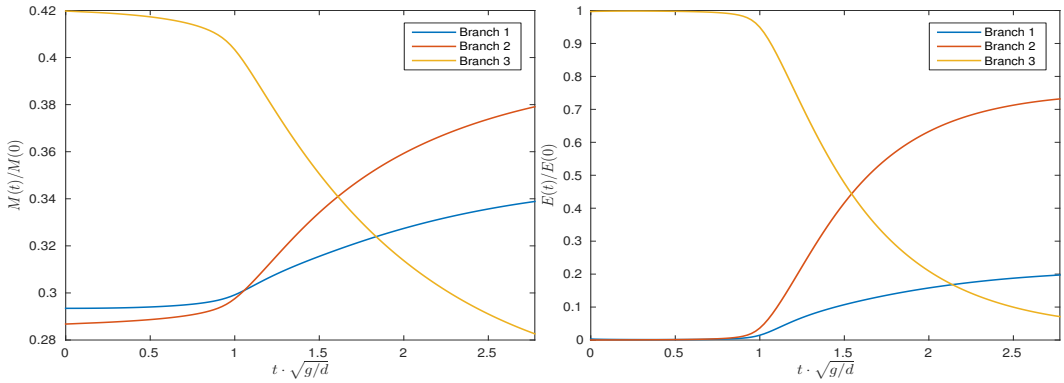


**Figure 6.** *Time evolution of the wave mass $M_w$ (left) and the wave energy $E_w$ (right) for a wave incident in branch* 3.

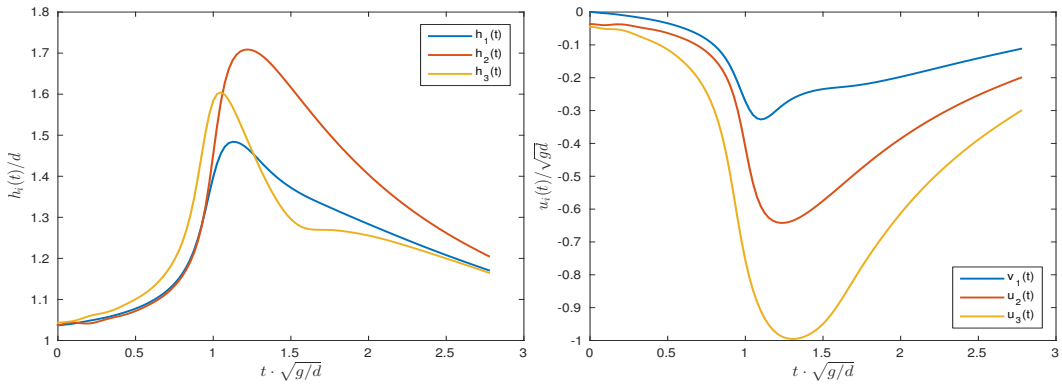


**Figure 7.** *Time evolution of the wave heights $h_1$, $h_2$, $h_3$ (left) and the wave speeds $v_1$, $u_2$, $u_3$ for a wave incident in branch* 3 .

in the $y$ component of the momentum is computed from the numerical solution. It is plotted as a function of time together with the estimate

$$h_{23}^2 \approx \frac{1}{2}\,(h_2^2 + h_3^2)\,,$$

in Fig. 8. As can be seen, the agreement is very good.

The correspondence between the 2D solution and the 1D effective solution is summarized in the Table 3. There we report the values of $\delta m$, $\delta p_x$, $\delta p_y$ and $\delta e$ from equations (6.4) – (6.7). These have been normalized by the initial mass, momenta and energy which are respectively

$$M = 1.77\,, \quad P_x = 1.28\,, \quad P_y = 1.02\,, \quad E = 2.37\,.$$

Table 3 shows that the relations (6.4) – (6.7) hold well except at $t = 1$ and $t = 1.25$ for the $u$ momentum and energy.

Let us now extract the coupling conditions from the relations (6.4) – (6.7). As mentioned above, a naturally small parameter is $v_1$ ; $h_2$ can be considered large. Then from the $v$

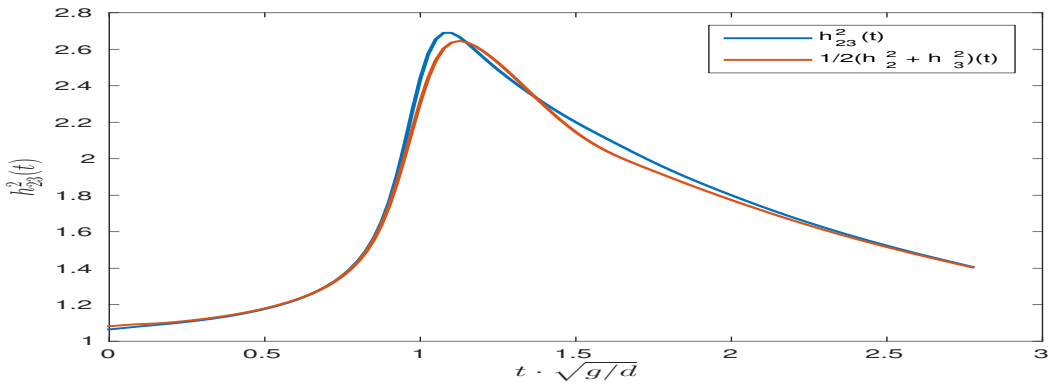


**Figure 8.** *Time evolution of the quantity* $h_{23}^2$ *from (6.13) together with* $\frac{1}{2}\,(h_2^2 \,+\, h_3^2)$ *.*

| *time* | $\delta m/M$ | $\delta p_x/P_x$ | $\delta p_y/P_y$ | $\delta e/E$ |
|---|---|---|---|---|
| 0.75 | -0.03 | 0.10 | 0.02 | -0.04 |
| 1 | -0.12 | 0.66 | 0.06 | -0.27 |
| 1.25 | 0.02 | 0.28 | 0.08 | -0.009 |
| 1.5 | 0.002 | 0.14 | 0.06 | -0.003 |
| 1.8 | 0.02 | 0.07 | 0.01 | 0.02 |
| 2.5 | 0.01 | 0.02 | 0.001 | 0.008 |

**Table 3.** *The mass, momentum and energy residuals* $\delta m$*,* $\delta e$ *in the equations (6.4) – (6.7) for different times.*

momentum (6.6) we get

$$h_1^2 \;=\; \frac{h_2^2 \,+\, h_3^2}{2}\,. \tag{6.14}$$

From the mass relation (6.4) we obtain

$$v_1 \;=\; \frac{h_3\,u_3 \;-\; h_2\,u_2}{h_1}\,. \tag{6.15}$$

From the $u$ momentum (6.5) we get,

$$\frac{g h_2^2}{2} \;+\; h_2\,u_2^2 \;=\; h_3\,u_3^2 \;+\; \frac{g h_3^2}{2}\,. \tag{6.16}$$

Consider the energy equation (6.7) and notice that $h^2 \;\gg\; u^2$. Then it can be simplified to

$$-v_1\,g\,h_1^2 \;-\; u_2\,g\,h_2^2 \;+\; u_3\,g\,h_3^2 \;=\; 0\,,$$

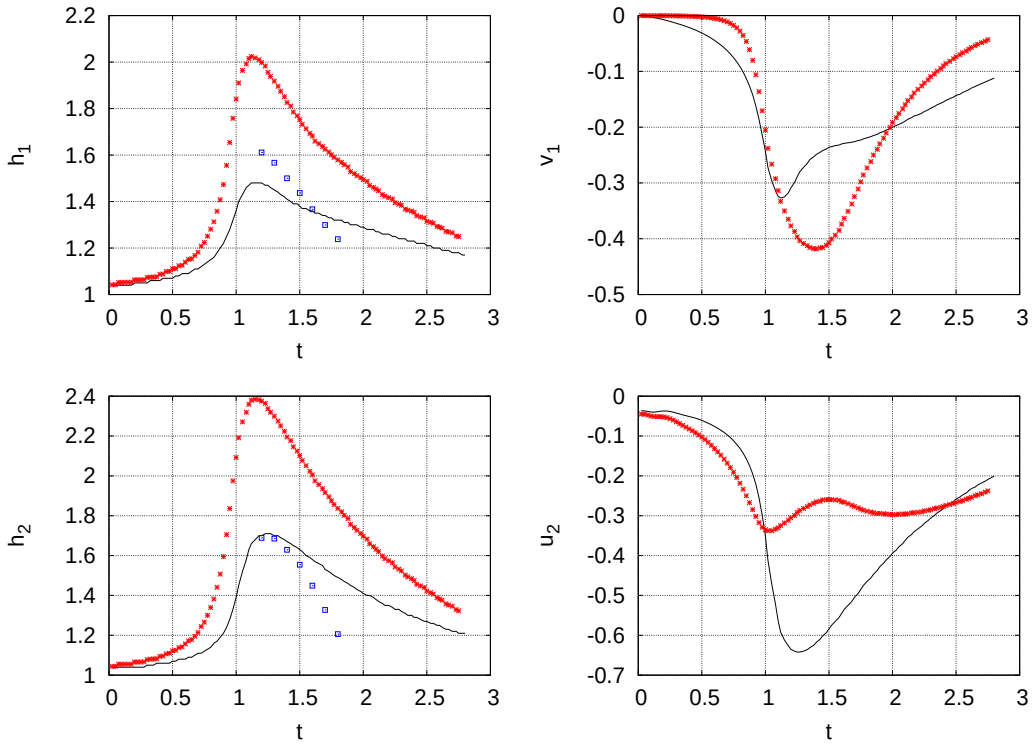


**Figure 9.** *Time evolution of $h_1$ (top left), $v_1$ (top right), $h_2$ (bottom left) and $u_2$ (bottom right) for a wave incident in branch 3. The values from the 2D simulation are drawn in continuous line (black online), the solutions of (6.17) calculated by* Newton–Raphson *are drawn with crosses (red online) and the solutions found by Maple are drawn with squares (blue online).*

To summarize, the nonlinear system that needs to be solved for $h_2$, $u_2$, $v_1$, $h_1$ is

$$v_1 = \frac{h_3\,u_3 - h_2\,u_2}{h_1}\,, \tag{6.17}$$

$$g\,h_2^2 + 2\,h_2\,u_2^2 = g\,h_3^2 + 2\,h_3\,u_3^2\,, \tag{6.18}$$

$$h_1 = \sqrt{\frac{h_2^2 + h_3^2}{2}}\,, \tag{6.19}$$

$$(h_2\,u_2 - h_3\,u_3)\,h_1 - u_2\,h_2^2 + u_3\,h_3^2 = 0\,, \tag{6.20}$$

where the $v$ momentum equation (6.6) has been used to obtain $h_1$, assuming $|v_1| < 1 < h_1$.

We have solved the nonlinear system (6.17) using Newton–Raphson. At each snapshot of the simulation, we used the values of $h_3$, $u_3$ from the 2D solution and took as initial guess, the solution obtained at the previous time. The time evolutions of $h_1$, $v_1$, $h_2$, $u_2$ are shown in Fig. 9. As can be seen the agreement is qualitatively good. On these plots are

also reported, solutions of (6.17) obtained using `Maple` software. Clearly, our estimates of $u_2$ are off as can be expected from the $\delta p_x$ column of Table 3.

## 6.3. Wave incident into branch 1 for a $Y-$geometry

To complete the validation of the conservation laws, we consider a $Y-$fork where $\theta_3 = \pi/4$ and $\theta_2 = 3\pi/4$. Then we have to consider the mass and energy equations (5.3) together with the momenta equations (5.7), (5.8). Assuming the symmetry $h_2 = h_3$, $u_2 = u_3$, the $u$ momentum conservation is automatically satisfied. We assume that contributions from the transverse sides $AB$, $HI$ balance out. Collecting the vertical momentum equation, energy and mass equations gives the following system

$$-(h_1 u_1^2) + 2(h_2 u_2^2 + g\frac{h_2^2}{2})\sin\theta_2 = 0,, \tag{6.21}$$

$$-u_1(g h_1^2 + h_1\frac{u_1^2}{2}) + 2u_2(g h_2^2 + h_2\frac{u_2^2}{2}) = 0, \tag{6.22}$$

$$-h_1 u_1 + 2 h_2 u_2 = 0, \tag{6.23}$$

where the $\|$ symbol has been omitted for simplicity. This is an interesting situation because we have two unknowns $h_2$, $u_2$ and three equations. Clearly, there is a problem of compatibility and one needs to choose two of the three conditions.

Picking mass and energy, we need to solve

$$u_2^3 - u_2(2 g h_1 + u_1^2) + g u_1 h_1 = 0, \tag{6.24}$$

$$h_2 = \frac{u_1 h_1}{2 u_2}. \tag{6.25}$$

which can be solved approximately as

$$h_2 = h_1 + \frac{u_1^2}{2g}, \qquad u_2 = \frac{g u_1 h_1}{2g h_1 + u_1^2}. \tag{6.26}$$

Similarly for mass and momentum, the relations are

$$4 u_2^3 u_1 \sin\theta - 2 u_2^2(2 u_1^2 + g h_1) + g \sin\theta h_1 u_1^2 = 0,$$

$$h_2 = \frac{u_1 h_1}{2u_2},$$

whose approximate solution is

$$h_2 = \frac{h_1}{2}\sqrt{\frac{4 u_1^2}{g\sin\theta h_1} + \frac{2}{\sin\theta}}, \qquad u_2^2 = \frac{g\sin\theta h_1 u_1^2}{4u_1^2 + 2 g h_1}. \tag{6.27}$$

Fig. 10 gives these estimates obtained from the conservation laws, energy-mass (top) momentum–mass (bottom), together with the ones from the 2D solution. Clearly, the energy gives better results than the momentum. This is reminiscent of the evolution of the soliton amplitude for the perturbed Korteweg–de Vries equation. There, Caputo &

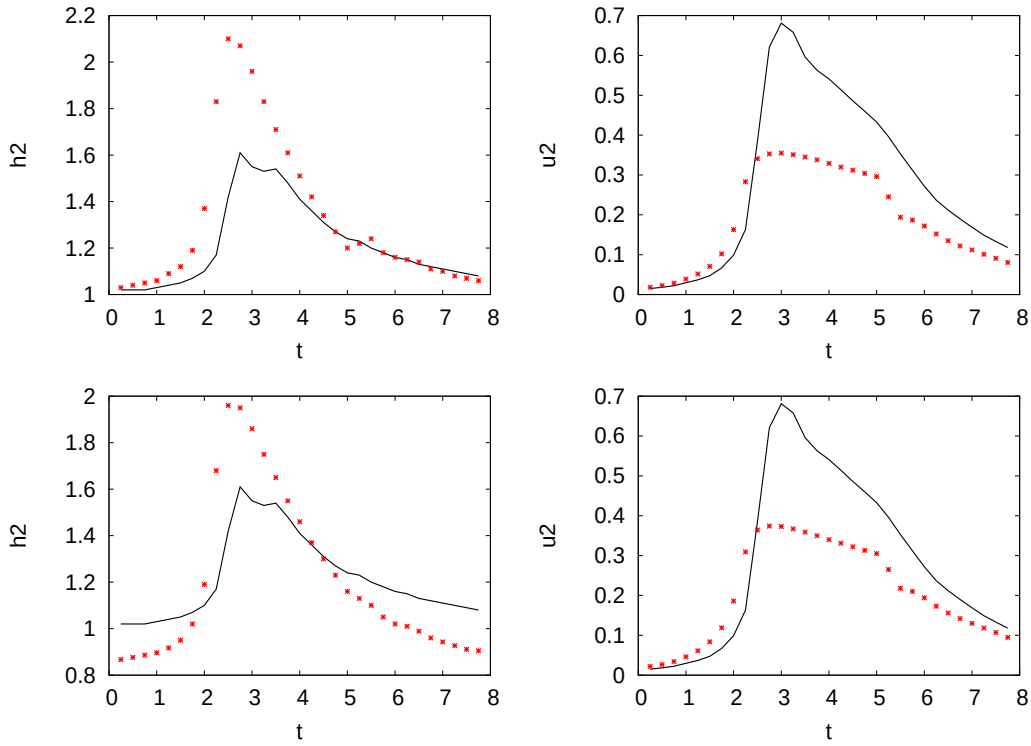


**Figure 10.** *Time evolution of $h_2$, $u_2$ a wave incident in branch 1 in a $Y-$fork. The top panels are obtained from the energy and mass conditions (6.22), (6.23) and the bottom panels from the momentum and mass conditions (6.21), (6.23). The values from the 2D simulation are drawn in continuous line (black online) while the estimates are in dashed line (red online)*

Stepanyants [3] show that the mass relation does not give the correct dependance while the energy relation does.

## 7. Conclusion

We studied the propagation of waves in a fork systematically using a homothetic reduction procedure that gives coupling conditions at the interface for an effective 1D PDE.

A nonlinear scalar wave equation like the 2D sine–Gordon or the 2D reaction diffusion equation naturally reduces to a 1D effective model. The coupling conditions are (i) continuity of the solution and (ii) continuity of the gradient (Kirchoff's law). For these equations, the angle of the 2D branch is irrelevant, it does not affect the dynamics and there is always 50% of the energy that is transmitted to each branch. This is apparent in the 1D effective model.

For the nonlinear shallow water equations the angle of the branches is very important as shown in the simulations for the $T-$branch. We considered the 2D numerical solution

and our reduction of the mass, momentum and energy laws on the fork region. The latter provide estimates of the unknown quantities in the outgoing branches. We showed that these estimates agree semi-quantitatively with the full 2D numerical solution.

An interesting result is that in some cases, like for the $Y-$branch, there are more conditions to satisfy than unknowns. Then one needs to choose which condition to use. For the $Y-$branch, mass and energy are a better choice than mass and vertical momentum.

It is remarkable that the equations (5.3), (5.7), (5.8) are exactly the jump conditions for a stationary shock, see [18]. Although our approach assumed subsonic waves and was tested on these, it would be interesting to see what happens for shocks.

## Acknowledgments

The authors thank Robert Indyk, Miguel Manna and Tim Minzoni for useful discussions. D. Dutykh acknowledges the support of CNRS through the project PEPS InPhyNiTi "FARA".

## References

[1] N. Bellomo and C. Dogbe. On the Modeling of Traffic and Crowds: A Survey of Models, Speculations, and Perspectives. *SIAM Review*, 53(3):409–463, jan 2011. 5

[2] J.-G. Caputo and D. Dutykh. Nonlinear waves in networks: model reduction for sine-Gordon. *Phys. Rev. E*, 90:022912, 2014. 5, 6, 8, 10

[3] J.-G. Caputo and Y. A. Stepanyants. Bore formation, evolution and disintegration into solitons in shallow inhomogeneous channels. *Nonlin. Processes Geophys.*, 10(4/5):407–424, 2003. 22

[4] R. M. Colombo and M. Garavello. On the Cauchy Problem for the p -System at a Junction. *SIAM J. Math. Anal.*, 39(5):1456–1471, jan 2008. 5

[5] D. Dutykh, D. Clamond, P. Milewski, and D. Mitsotakis. Finite volume and pseudo-spectral schemes for the fully nonlinear 1D Serre equations. *Eur. J. Appl. Math.*, 24(05):761–787, 2013. 13

[6] D. Dutykh, R. Poncet, and F. Dias. The VOLNA code for the numerical modeling of tsunami waves: Generation, propagation and inundation. *Eur. J. Mech. B/Fluids*, 30(6):598–615, 2011. 13

[7] J. Hadamard. *Leçons sur la géométrie élémentaire*. Librairie Armand Colin, Paris, 1906. 8

[8] M. Herty and M. Seaïd. Assessment of coupling conditions in water way intersections. *Int. J. Num. Meth. Fluids*, 71(11):1438–1460, apr 2013. 5

[9] H. Holden and N. H. Risebro. Riemann Problems with a Kink. *SIAM J. Math. Anal.*, 30(3):497–515, jan 1999. 5

[10] P. M. Jacovkis. One-Dimensional Hydrodynamic Flow in Complex Networks and Some Generalizations. *SIAM J. Appl. Math*, 51(4):948–966, 1991. 5

[11] L. D. Landau and E. M. Lifshitz. *Fluid Mechanics*. Pergamon Press, Oxford, 2nd edition, 1987. 5

[12] A. Nachbin and V. S. Simões. Solitary waves in forked channel regions. *J. Fluid Mech.*, 777:544–568, aug 2015. 5

[13] E. J. P. G. Schmidt. On Junctions in a Network of Canals. In O. Imanuvilov, G. Leugering, R. Triggiani, and B.-Y. Zhang, editors, *Control Theory of Partial Differential Equations*, pages 207–212. Chapman & Hall/CRC, Boca Raton, FL, 2005. 5

[14] F. Serre. Contribution à l'étude des écoulements permanents et variables dans les canaux. *La Houille blanche*, 8:374–388, 1953. 13

[15] F. Serre. Contribution à l'étude des écoulements permanents et variables dans les canaux. *La Houille blanche*, 8:830–872, 1953. 13

[16] L. F. Shampine and M. W. Reichelt. The MATLAB ODE Suite. *SIAM Journal on Scientific Computing*, 18:1–22, 1997. 13

[17] J. J. Stoker. *Water waves, the mathematical theory with applications*. Wiley, 1958. 5, 6

[18] G. B. Whitham. *Linear and nonlinear waves*. John Wiley & Sons Inc., New York, 1999. 23

Laboratoire de Mathématiques, INSA de Rouen, BP 8, Avenue de l'Université, Saint-Etienne du Rouvray, 76801 France

*E-mail address*: caputo@insa-rouen.fr

*URL*: https://sites.google.com/site/jeanguycaputo/

LAMA, UMR 5127 CNRS, Université Savoie Mont Blanc, Campus Scientifique, 73376 Le Bourget-du-Lac Cedex, France

*E-mail address*: Denys.Dutykh@univ-savoie.fr

*URL*: http://www.lama.univ-savoie.fr/~dutykh/

Laboratoire de Mathématiques, INSA de Rouen, BP 8, Avenue de l'Université, Saint-Etienne du Rouvray, 76801 France

*E-mail address*: gleyse@insa-rouen.fr